Supporting Imformation

Metal-Organic Frameworks with Large Breathing Effect to Host Hydroxyl Compounds for High Anhydrous Proton Conductivity over a Wide Temperature Range from Subzero to 125 °C

Yingxiang Ye,[#], [a] Xiuzhen Wu, [#], [a] Zizhu Yao,[a] Ling Wu,[a] Zetao Cai,[a] Lihua Wang,[a] Xiuling Ma,[a] Qian-Huo Chen,[a] Zhangjing Zhang,*, [a] and Shengchang Xiang,*, [a]

[a] *College of Materials Science and Engineering, Fujian Provincial Key Laboratory of Polymer Materials, Fujian Normal University, 32 Shangsan Road, Fuzhou 350007, P R China. E-mails: zzhang@fjnu.edu.cn; scxiang@fjnu.edu.cn*

[#] *These authors contributed equally to this work.*

Content

Table S1 | Crystallographic data and structure refinement results……....S3

Table S2 | Guest-induced breathing effect amplitudes of reported compounds.....S5

Table S3 | The comparison of proton conductivity on **FJU-31@Hq** and **FJU-31@Ch** with representative crystalline porous proton-conductor materials.…….……S7

Figure S1 | Supplementary structural figure for **FJU-30**…….…..…..…S10

Figure S2 | The PXRD patterns for the as-synthesized samples..…….....S11

Figure S3 | The TGA curves for the as-synthesized MOFs…….....…..S12

Figure S4 | The significant difference dihedral angle in **FJU-31** and **FJU-31@Bu**…….....S13

Figure S5 | The evolution of the 1D rhombic channel in **FJU-31@Hq** and **FJU-31@Ch**….....S13

Figure S6 | FT-IR spectra for the as-synthesized MOFs…….…….….…..S14

Figure S7 | The DSC profiles for **FJU-31@Hq** and **FJU-31@Ch**…….....…….....S15

Figure S8 | N_2 sorption isotherms at 77 K for **FJU-31**…….……...……...….....S16

Figure S9 | CO_2 sorption isotherms for **FJU-31**……...…...…….....S16

Figure S10 | Nyquist plots for **FJU-31@Hq** at different temperatures……..S17

Figure S11 | Nyquist plots for **FJU-31@Ch** at different temperatures…….……..S18

Figure S12 | Nyquist plots for **FJU-31@Bu** at different temperatures…….……..S19

Figure S13 | Fitting for the Nyquist plot at 30°C of **FJU-31@Hq**.....…….S20

Figure S14 | Arrhenius plot for **FJU-31@Hq** and **FJU-31@Ch** in comparison with other representative proton-conducting materials under anhydrous conditions..……...S21

Figure S15 | Speculative proton-conducting pathways for **FJU-31@Hq** and **FJU-31@Ch**….....S22

Supplementary References……..…….……..S23

Table S1 | Crystal data and refinement results for the as-synthesized samples.

Identification code	**FJU-30**	**FJU-31**	**FJU-31@Hq-lt**	**FJU-31@Hq**
CCDC	1442065	1442071	1442067	1442066
Empirical formula	$C_{12}H_{12}N_{22}O_{12}Zn_5$	$C_{20}H_{12}N_6O_8Zn_3$	$C_{34}H_{36}N_8O_{12}Zn_3$	$C_{20}H_{12}N_6O_8Zn_3$
Formula weight	983.29	660.47	944.82	660.47
Temperature/K	293(2)	293(2)	100	293(2)
Crystal system	tetragonal	monoclinic	triclinic	monoclinic
Space group	$I4_1/a$	$P2_1/c$	P-1	$C2/m$
a/Å	15.5031(4)	8.6854(5)	9.1768(5)	11.9442(16)
b/Å	15.5031(4)	19.7877(8)	10.9017(8)	19.1318(10)
c/Å	12.0934(4)	7.9849(5)	11.3961(9)	9.2109(7)
α/°	90	90	117.938(8)	90
β/°	90	113.775(7)	100.535(5)	109.821(12)
γ/°	90	90	98.517(5)	90
V/Å^3	2906.58(17)	1255.86(13)	953.72(13)	1980.1(4)
Z	4	2	1	2
ρ_{calc} g/cm^3	2.247	1.747	1.645	1.108
M /mm^{-1}	5.503	3.845	2.829	2.439
F(000)	1936.0	656.0	482.0	656.0
Crystal size/mm^3	0.12 × 0.06 × 0.06	0.2 × 0.1 × 0.1	0.15 × 0.1 × 0.1	0.15 × 0.1 × 0.1
Radiation	Cu $K\alpha$ (λ = 1.54184Å)	Cu $K\alpha$ (λ= 1.54184 Å)	Cu $K\alpha$ (λ= 1.54184 Å)	Cu $K\alpha$ (λ= 1.54184 Å)
Goodness-of-fit on F^2	1.040	1.008	1.021	0.968
Final R indexes [I>=2σ (I)][a]	R_1= 0.0320, wR_2= 0.0781	R_1= 0.0420, wR_2= 0.1009	R_1= 0.0810, wR_2= 0.2161	R_1= 0.0430, wR_2= 0.1000
Final R indexes [all data][a]	R_1= 0.0402, wR_2= 0.0847	R_1= 0.0608, wR_2= 0.1119	R_1= 0.0956, wR_2= 0.2326	R_1= 0.0640, wR_2= 0.1099
Largest diff. peak/hole / e Å^{-3}	0.37/-0.35	0.61/-0.49	1.95/-1.05	0.53/-0.43

Identification code	**FJU-31@Ch-lt**	**FJU-31@Ch**	**FJU-31 @Bu**
CCDC	1442069	1442068	1442070
Empirical formula	$C_{38}H_{47}N_6O_{11}Zn_3$	$C_{20}H_{12}N_6O_8Zn_3$	$C_{20}H_{12}N_6O_8Zn_3$
Formula weight	959.92	660.47	660.47
Temperature/K	100	293(2)	293(2)
Crystal system	triclinic	triclinic	monoclinic
Space group	*P*-1	*P*-1	*C2/m*
a/Å	9.1743(4)	9.2142(6)	12.1742(4)
b/Å	10.8488(5)	11.1531(19)	18.9858(5)
c/Å	11.3458(5)	11.3582(19)	9.1980(3)
α/°	113.479(4)	112.294(16)	90
β/°	98.726(4)	99.494(9)	108.810(4)
γ/°	98.016(4)	99.046(9)	90
V/Å^3	998.57(8)	1033.8(3)	2012.46(11)
Z	1	1	2
ρ_{calc} mg/mm^3	1.596	1.061	1.090
M /mm^{-1}	2.674	2.336	2.400
F(000)	495.0	328.0	656.0
Crystal size/mm^3	0.2 × 0.15 × 0.1	0.2 × 0.15 × 0.1	0.2 × 0.15 × 0.1
Radiation	Cu *Kα* (λ= 1.54184 Å)	Cu *Kα* (λ= 1.54184 Å)	Cu *Kα* (λ= 1.54184 Å)
Goodness-of-fit on F^2	1.047	1.017	1.079
Final R indexes [I>=2σ (I)][a]	R_1= 0.0670, wR_2= 0.1850	R_1= 0.0835, wR_2= 0.1996	R_1= 0.0255, wR_2= 0.0748
Final R indexes [all data][a]	R_1= 0.0740, wR_2= 0.1937	R_1= 0.1124, wR_2= 0.2213	R_1= 0.0284, wR_2= 0.0769
Largest diff. peak/hole / e Å^{-3}	1.91/-1.10	2.56/-0.90	0.27/-0.39

(a) $R_1 = \sum ||F_O| - |F_C|| / \sum |F_O|$; $wR_2 = [\sum w(|F_O|^2 - |F_C|^2)^2 / \sum w(F_O^2)^2]^{1/2}$

Table S2 | Guest-induced breathing amplitudes (BA, %) of reported compounds.

Compounds	Phase	Space group	*a* (Å)	*b* (Å)	*c* (Å)	V_{cell}/Z (Å^3)	BA (%)	Tools	Ref.
[Mn(pba)$_2$]	close	*I2/a*	8.5203	15.0866	18.313	2331.4/4		SCXRD	1
	DMF	*I2/a*	8.5876	14.9686	18.6280	2380.6/4	2.1		
	DMA	*I2/a*	8.721	14.945	18.656	2420/4	3.8		
[CdL$_2$(ClO$_4$)$_2$]	close	*P*6$_2$22	19.254	19.254	28.326	9094.2/3		SCXRD	2
	open	*P*6$_2$22	19.477	19.477	28.277	9289.8/3	2.2		
Zn (34pba)$_2$	close	*P*4$_3$2$_1$2	11.5806	11.5806	34.904	4681.0/8		SCXRD	3
	propanol	*P*4$_3$2$_1$2	11.6638	11.6638	36.790	5005.0/8	6.9		
	butanol	*P*4$_3$212	11.728	11.728	36.977	5086/8	8.6		
`[Zn$_2$(fu-bdc)$_2$ (dabco)]$_n$	9-close	*C2/m*	19.12	9.00	9.00	1658/2		PXRD	4
	9-DMF	*I4/mcm*	15.44	15.44	19.26	4593/4	38.5		
	8-close	*C2/m*	18.91	9.92	9.57	1789/2			
	8-DMF	*P4/mmm*	10.94	10.94	9.64	1154/1	29.0		
Cu(BDTri)L	close	*Imma*	24.561	6.9860	9.1333	1567.1/4		SCXRD	5
	open	*Imma*	22.538	7.044	13.772	2186.5/4	39.5		
MIL-53	close	*C2/c*	19.685	7.849	6.782	1012.8/4		in situ PXRD	6
	H$_2$BDC	*Pnam*	17.340	12.178	6.822	1440.6/4	42.2		
	open	*Imcm*	16.733	13.038	6.812	1486.1/4	46.7		
COMOC-2	close		6.651	27.94	10.735	1979.4		PXRD	7
	open	*Imma*	6.776	23.087	18.897	2956.1	49.3		
FJU-31	close	*P*2$_1$/*c*	8.6854	19.7877	7.9849	1255.86/2		SCXRD	**this work**
	Hq	*C2/m*	11.9442	19.1318	9.2109	1980.1/2	62		
	Ch	*P*-1	9.2142	11.1531	11.3582	1033.8/1	65		
	Bu	*C2/m*	1033.8	18.9858	9.1980	2012.46/2	60		
MCF-18(L3,Ni)	close	*R-3c*	29.792	29.792	12.063	9271/6		SCXRD	8
	Pyridine	*R-3c*	28.691	28.691	26.622	18986/6	105		
	DMF	*R-3c*	28.948	28.948	24.341	17664/6	90		
	DMA	*R-3c*	28.932	28.932	23.920	17339/6	87		
Co(BDP)	close	*C2/c*	24.87	6.04	7.22	1084		in situ PXRD	9
	Int.3	*C2/c*	21.61	15.55	7.02	2338	116		
	Filled	*P*4$_1$22	13.29	13.29	14.82	2618	142		
MIL-88A	close	*P-62c*	9.26	9.26	15.31	1135/2			10
	CH$_3$OH	*P-62c*	13.78	13.78	12.69	2090/2	84.1		
	H$_2$O	*P-62c*	13.87	13.87	12.66	2110/2	85.9		
MIL-88B	close	*P*6$_3$/mmc	9.5	9.5	19.0	1485/1		in situ PXRD	11
	CH$_3$OH	*P*6$_3$/mmc	15.626	15.626	15.960	3375.0/1	127		
MIL-88C	close	*P*-62c	10.0	10.0	23.2	2120			12
	Pyridine	*P*-62c	18.753	18.753	18.743	5708.2/1	169.2		
MIL-88D	close	*P*-62c	10.2	10.2	27.6	2490/1			11,12
	Lutidine	*P*-62c	20.040	20.040	22.911	7968.7/1	220		
MIL-89	close	*Pbnn*	9.13	9.13	20.0	1470/1		in situ PXRD	13
	Pyridine	*P*6$_3$/*mmc*	17.0	17.0	15.7	3900/1	165		
	Methanol	*P*6$_3$/*mmc*	15.8	15.8	16.75	3615/1	146		

Amplitudes of breathing (BA, %) for the crystal structures above, corresponding to the structural switching from the open to the closed forms, are calculated from the equation $100\times(V_{op}-V_{dry})/V_{dry}$. V was derived from the unit cell volumes (V_{cell}) and the number of formula units per unit cell (Z) according to the following equation: $V = V_{cell}/Z$.

Table S3 | The comparison of proton conductivity on **FJU-31@Hq** and **FJU-31@Ch** with representative proton conductor materials. The compounds in the first part with white background are tested in anhydrous conditions, those in the second part with cyan background measured under moist conditions.

Compounds	Guests	Proton Conductivity (S cm^{-1})				temperature range of the test (°C)	E_a (eV)	Ref
		-30 °C	30 °C	120 °C	Max (T)			
$\{[(Me_2NH_2)_3(SO_4)]_2[Zn_2(ox)_3]\}_n$	$(Me_2NH_2)^+$, SO_4^{2-}		7×10^{-5}	1×10^{-4}	1×10^{-4} (150 °C)	30~150	0.13	14
FJU-31@Hq	Hq, DMAc	1.49×10^{-5}	5.42×10^{-5}	2.47×10^{-4}	2.65×10^{-4} (125 °C)	-40~125	0.18	**This work**
FJU-31@Ch	Ch	2.36×10^{-6}	2.11×10^{-5}	8.05×10^{-5}	8.05×10^{-5} (120 °C)	-40~120	0.19/ 0.29	**This work**
His @ $[Al(OH)(1,4\text{-ndc})]_n$	His		3.85×10^{-5}	1.06×10^{-3}	1.7×10^{-3} (150 °C)	25~150	0.25	15
$[Eu_2(CO_3)(ox)_2(H_2O)_2]\cdot4H_2O$	H_2O		9.48×10^{-6}	1.18×10^{-3}	2.08×10^{-3} (150 °C)	25~150	0.28	16
Im@Td-PPI	Im	4.4×10^{-6}	7.64×10^{-5}		3.49×10^{-4} (90 °C)	-40~90	0.30	17
Im@Td-PNDI	Im	9.0×10^{-7}	2.26×10^{-5}		0.90×10^{-4} (90 °C)	-40~90	0.33	17
Im@UiO-67	Im			1.44×10^{-3}	1.58×10^{-3} (130 °C)	45~130	0.36	18
$[Zn_3(H_2PO_4)_6(H_2O)_3](Hbim)$	Hbim		1.40×10^{-7}		6.1×10^{-7} (60 °C)	30~60	0.4	19
$[Zn(HPO_4)(H_2PO_4)_2](ImH_2)_2$	ImH_2^+		4.71×10^{-8}	2.51×10^{-4}	2.6×10^{-4} (130 °C)	25~130	0.47	20
In-IA-2D-2	$(Me_2NH_2)^+$, DMF		2.33×10^{-5}		2.72×10^{-5} (77 °C)	25~90	0.48	21
$[Co_2Na(bptc)_2][Emim]_3$	$Emim^+$			7.83×10^{-8}	6.33×10^{-7} (170 °C)	70~170 along *c* axis	0.49	22
$[Zn_3(H_2PO_4)_6](Hbim)$	Hbim		1.20×10^{-7}	1.3×10^{-3}	1.3×10^{-3} (120 °C)	30~120	1.5/0.5	19
β-PCMOF2$(Tz)_{0.3}$	TzH		1.04×10^{-6}	1.35×10^{-4}	2×10^{-4} (150 °C)	23~150	0.51	23
$[Zn(H_2PO_4)_2(TzH)_2]_n$	TzH			5.01×10^{-5}	1.2×10^{-4} (150 °C)	45~150	0.6	24
Im@$\{Al(\mu_2\text{-OH})(1,4\text{-ndc})\}_n$	Im		2.56×10^{-7}	2.2×10^{-5}	2.2×10^{-5} (120 °C)	25~120	0.6	25
$[Zn(H_2PO_4)_2(HPO_4)]\cdot(H_2dmbim)_2$	H_2dmbim		1.22×10^{-9}	6.91×10^{-6}	2×10^{-4} (190 °C)	30~190	0.66	26
Im@$\{Al(\mu_2\text{-OH})(1,4\text{-bdc})\}_n$	Im		5.84×10^{-10}	1.0×10^{-7}	1.0×10^{-7} (120 °C)	25~120	0.9	25

$[ImH_2][Cu(H_2PO_4)_{1.5}(HPO_4)_{0.5}\cdot Cl_{0.5}]$	ImH_2^+	1.69×10^{-7}	9.31×10^{-3}	2×10^{-2} (130 °C)	25~130	1.1	27
$[Zn(H_2PO_4)_2(HPO_4)]\cdot H_2dabco$	H_2dabco		6.13×10^{-9}	8×10^{-5} (160 °C)	90~150	1.2	26
PA@Tp-Azo	H_3PO_4, H_2O	4.70×10^{-5}	4.93×10^{-5}	6.7×10^{-5} (67 °C)	22~136		28
His@Zn-MOF-74	His		7.32×10^{-11}	4.3×10^{-9} (146 °C)	40~146		29
PA@Tp-Azo	H_3PO_4, H_2O	4.7×10^{-5} 90% RH		9.9×10^{-4} 98% 59 °C	22~67	0.11	28
PCMOF-5	H_2O	1.56×10^{-3} 98% RH		2.51×10^{-3} 98% RH 60 °C	20~60	0.16	30
[MIL-53(Fe)$(COOH)_2$]	H_2O	3.62×10^{-6} 95% RH		7×10^{-6} 95% RH (80 °C)	20~80	0.21	31
nafion	H_2O	5×10^{-2} 98% RH		1×10^{-1} 98% RH 80 °C	25~80	0.22	32
$(NH_4)_4[MnCr_2(ox)_6]_3\cdot4H_2O$	H_2O, NH_4^+	1.35×10^{-3} 96% RH		1.7×10^{-3} 96% RH 40 °C	22~40	0.23	33
H_3PO_4@MIL-101	H_3PO_4, little H_2O	2.06×10^{-4}	2.8×10^{-3} 20% RH	3×10^{-3} 0.13% RH 150 °C	30~150	0.25	34
UiO-66$(SO_3H)_2$	H_2O	1.8×10^{-2} 90% RH		8.4×10^{-2} 90% RH 80 °C	25~80	0.32	35
$[Zn(l\text{-}LCl)(Cl)](H_2O)_2$	H_2O	4.45×10^{-5} 98% RH		4.45×10^{-5} 98% RH 31 °C	23~31	0.34	36
$Fe(ox)\cdot2H_2O$	H_2O	2.79×10^{-3} 98% RH		3.23×10^{-3} 98% RH 45 °C	5~45	0.37	37
Cucurbit[6]uril·HCl (CB[6])	HCl, H_2O	3.82×10^{-4} 98% RH		1.3×10^{-3} 98% RH 40 °C	24~40	0.39	38
H_2SO_4@MIL-101	H_2SO_4, little H_2O		2.71×10^{-2} 20% RH	1×10^{-2} 0.13% RH 150 °C	40~150	0.42	34
$(NH_4)_2(adp)[Zn_2(ox)_3]\cdot3H_2O$	H_2O, NH_4^+	1.18×10^{-2} 98% RH		1.64×10^{-2} 98% RH 35 °C	25~35	0.63	39

Im=Imidazole; PA=H_3PO_4; Tp=triformylphloroglucinol; Azo= 4,4′-azodianiline; His=Histamine; 1,4-ndc=1,4-naphthalene dicarboxylic acid; $(Me_2NH_2)^+$=dimethyl ammonium; In-IA-2D-2= $\{In(IA)_2[(CH_3)_2NH_2](DMF)\}$; IA =isophthalic acid; ox= oxalate; *β*-PCMOF2= Na_3(2,4,6-trihydroxy-1,3,5-benzenetrisulfonate); TzH=1,2,4-Triazole; ImH_2^+=Imidazole cations; Hbim=Benzimidazole; H_2dmbim=5,6-dimethylbenzimidazole; 1,4-bdc=1,4-benzenedicarboxylic acid; $Emim^+$= 1-ethyl-3-methyl imidazolium; bptc= 2,2',4,4'-biphenyl tetracarboxylic; H_2dabco= 1,4-diazabicyclo[2.2.2]octane; Zn-MOF-74= $[Zn_2(2,5\text{-DOTP})]_n$ (DOTP = 2,5-dioxidoterephthalate); adp= adipic acid; PCMOF-5= $LaH_5L(H_2O)_4$ (L= Benzene-1,2,4,5-tetramethylenephosphonic acid); Hq=hydroquinone, Ch=cyclohexanol.

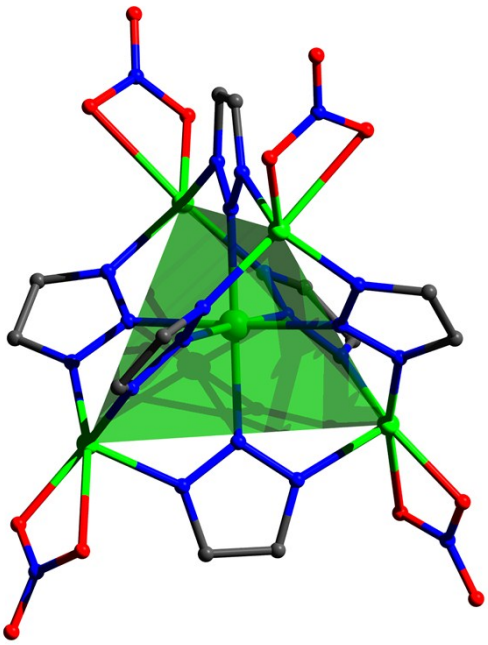

Figure S1 | The coordination geometry of the precursor $[Zn_5(tz)_6(NO_3)_4]$ **FJU-30**; Zinc polyhedron, carbon, nitrogen and oxygen atoms are green, gray, blue, and red, respectively, H atoms are omitted for clearly.

The pentanuclear precursor $Zn_5(tz)_6(NO_3)_4$ (**FJU-30**) is precipitated in colorless bulk crystals from ethanol solution of $Zn(NO_3)_2 \cdot 6H_2O$ and 1*H*-1,2,3-triazole at 100 ^oC for 1 day in a Teflon-lined steel bomb. It crystallizes in the tetragonal space group $I4_1/a$, composed of a tetrahedral arrangement of four five-coordinate Zn^{2+} ions centered on the fifth one. Each of the six tz ligands straddles an edge of the tetrahedron and is bound to the central metal through the nitrogen atom in the 2-position. Six nitrogen atoms from six tz ligands therefore complete the coordination sphere of the central Zn^{2+} ion, while each Zn^{2+} ion on the apical positions is coordinated by three nitrogen atoms from three tz ligands and two oxygen atoms from a chelating nitrate group.

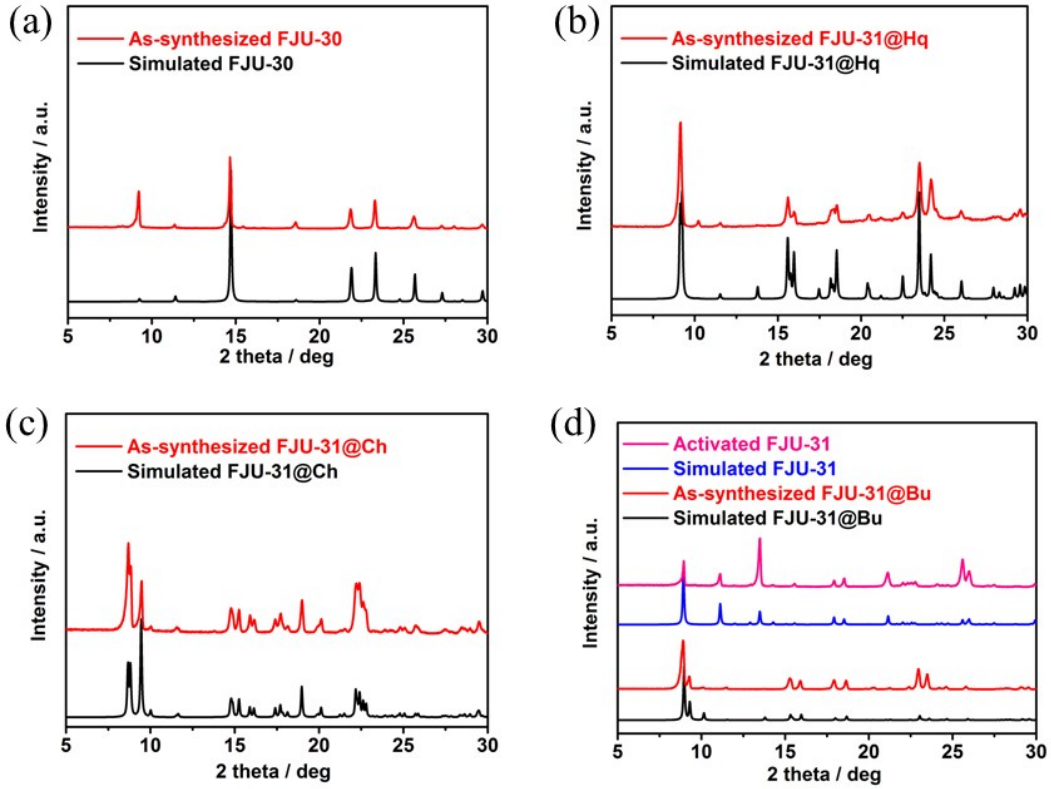

Figure S2 | PXRD patterns for the as-synthesized samples.

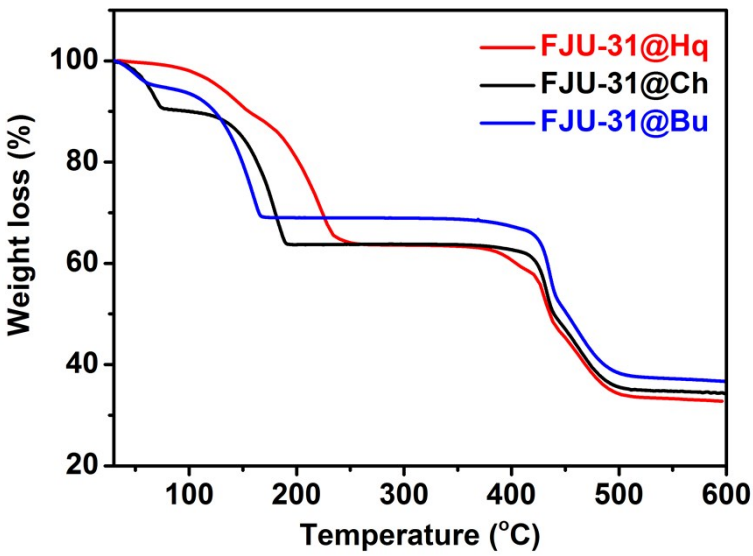

Figure S3 | TGA curves for **FJU-31@Hq**, **FJU-31@Ch** and **FJU-31@Bu**.

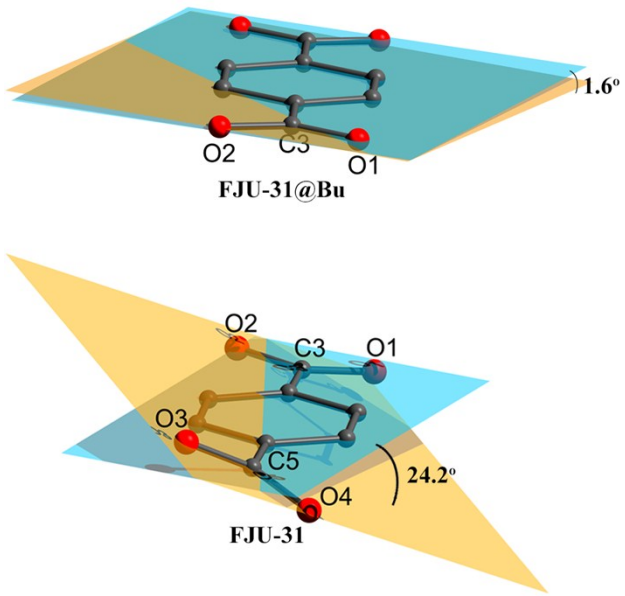

Figure S4 | The angles between the plane of carboxyl (light orange) and phenyl ring (light blue) are 1.6° and 24.2° in **FJU-31@Bu** and **FJU-31**, respectively.

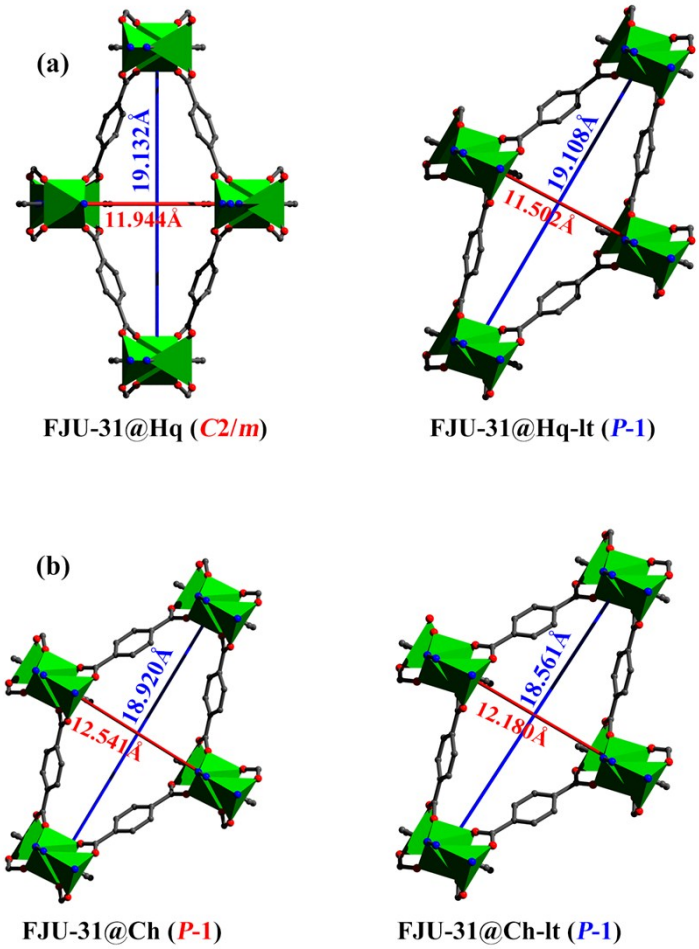

Figure S5 | Perspective view of the evolution of the 1D rhombic channel of **FJU-31@Hq** (a) and **FJU-31@Ch** (b) induced by the temperature stimulus.

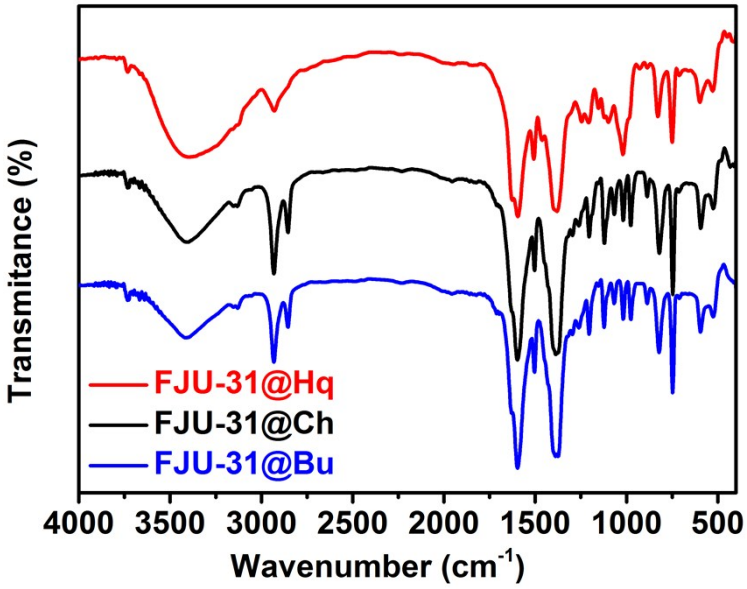

Figure S6 | FT-IR spectra for **FJU-31@Hq**, **FJU-31@Ch** and **FJU-31@Bu**.

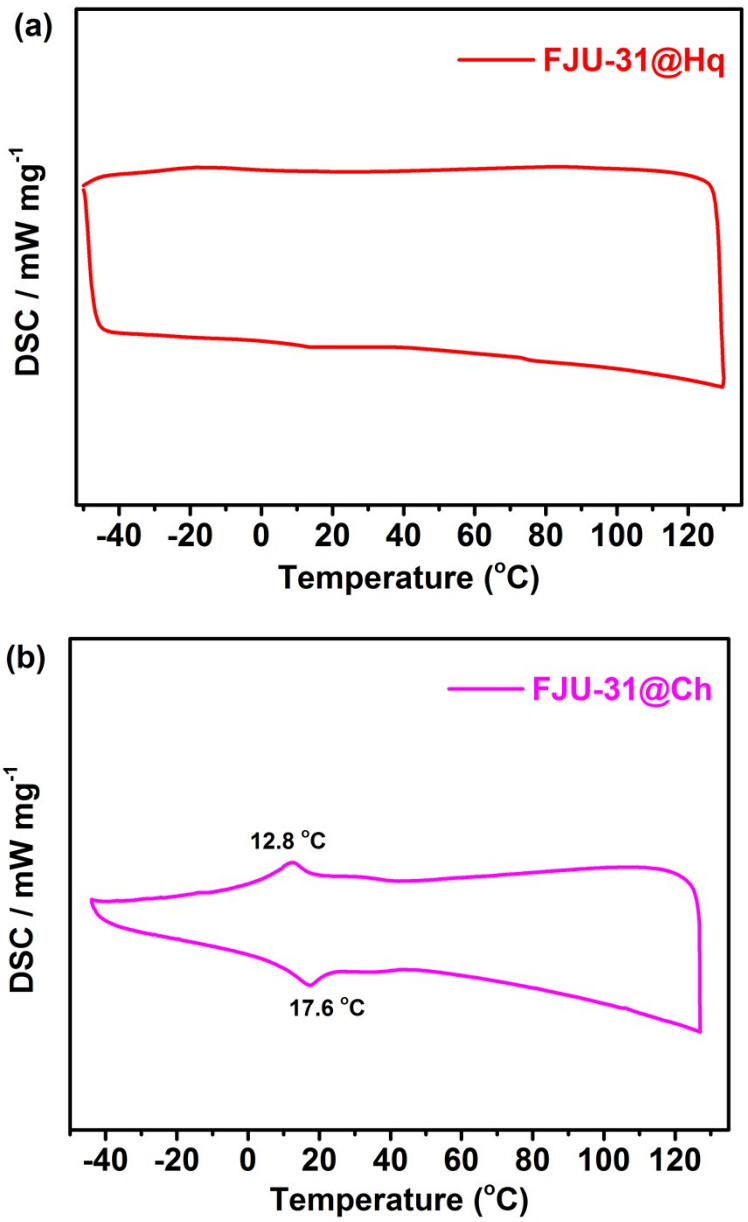

Figure S7 | The DSC profiles for **FJU-31@Hq** (a) and **FJU-31@Ch** (b).

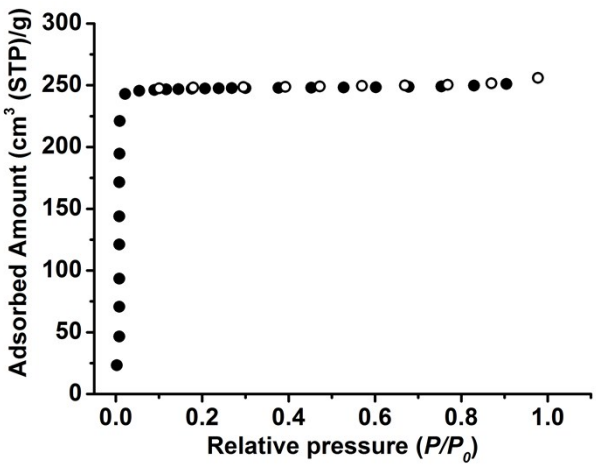

Figure S8 | N_2 sorption isotherms at 77 K for **FJU-31**.

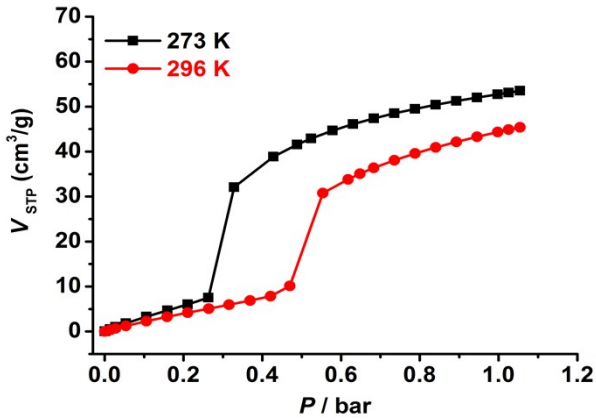

Figure S9 | CO_2 sorption isotherms for **FJU-31** at 273 K and 296 K.

In order to investigate the gas-sorption properties, **FJU-31@Bu** was exchanged by CH_2Cl_2 and then evacuated at room temperature 24 h in a vacuum to form the desolvated sample **FJU-31**. The 77 K N_2 sorption isotherms show type-I behaviors (**Figure S8**) and characterized typical crystalline microporous materials. The BET and Langmuir surface areas are 890.6 and 1132.5 m^2/g, respectively. Intriguing dynamic adsorption behavior is presented in the low pressure CO_2 isotherm of **FJU-31** recorded at 273 K and 296 K, respectively (**Figure S9**). The CO_2 isotherm at 273 K shows a sudden increase at P = 0.26 bar. Such step in the isotherm is due to structural changes during adsorption.[40] The atypical CO_2 adsorption behavior at 273 K encouraged us to further measure its CO_2 isotherm at room temperature. Notably, the adsorption step move to higher absolute pressure (P = 0.47 bar) with increasing temperature. The CO_2 uptake value of **FJU-31** at 273 K and 1 bar is 53 cm^3/g, compared with that of $Zn_3(tz)_2(bdc)_2{\cdot}x(DMF)$ (57 cm^3/g) reported by Zhang *et al.*[41]

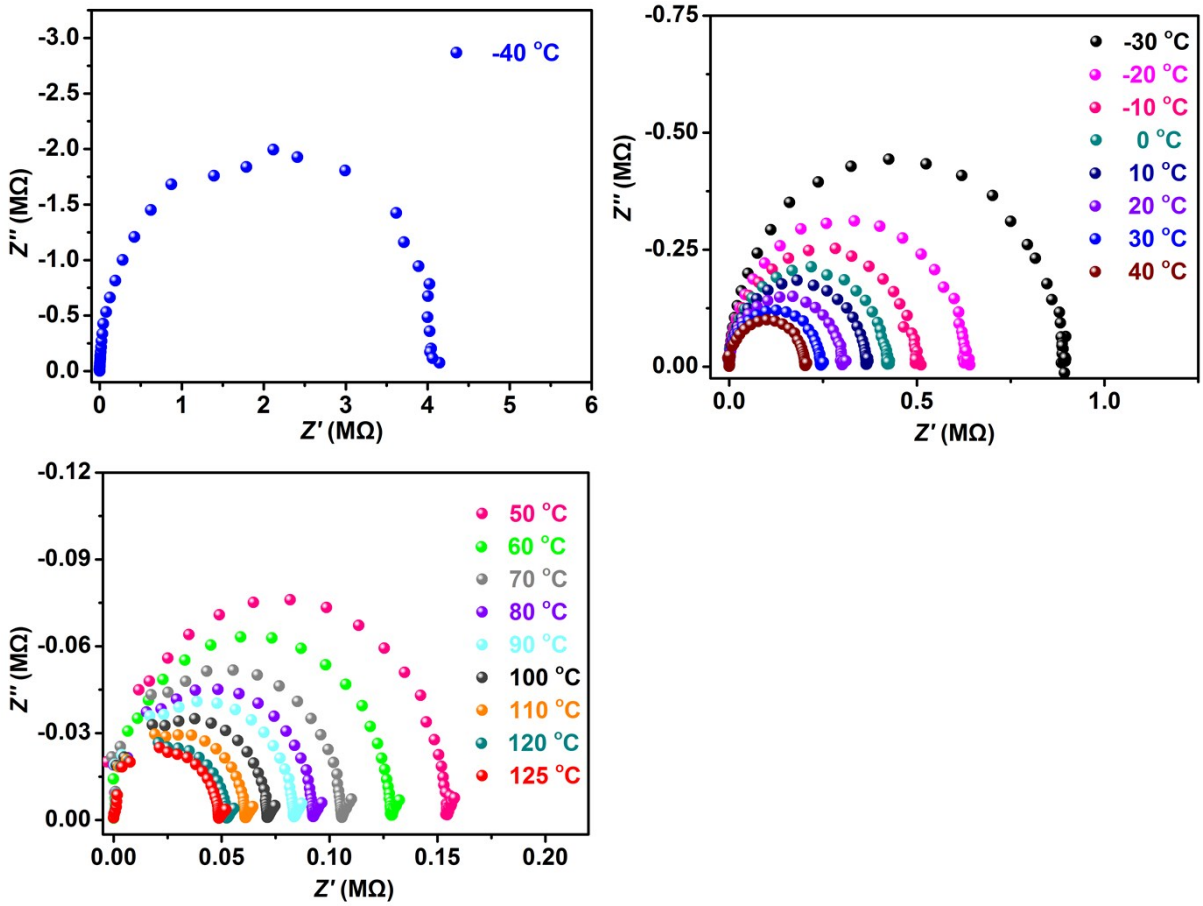

Figure S10 | Proton conductivity of **FJU-31@Hq** in anhydrous conditions at different temperature.

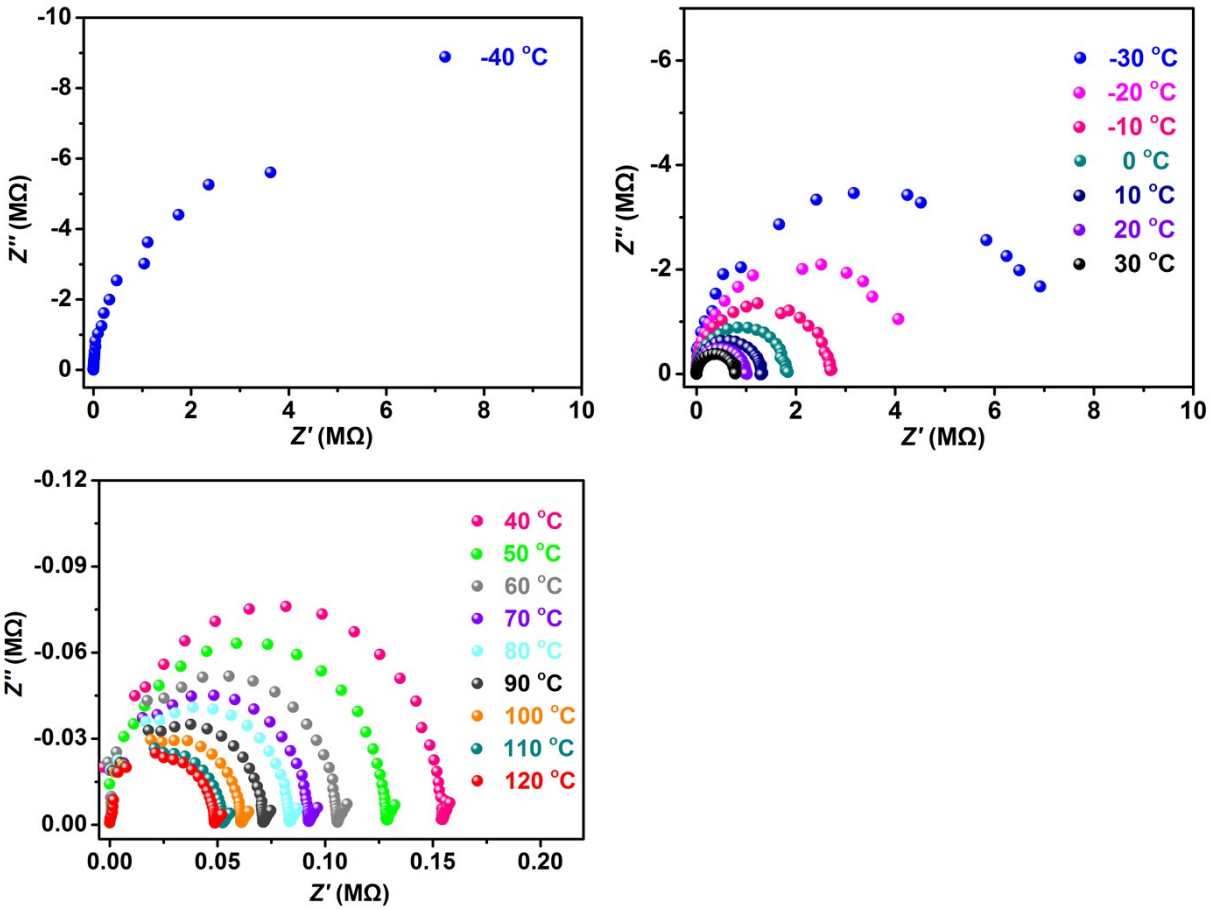

Figure S11 | Proton conductivity of **FJU-31@Ch** in anhydrous conditions at different temperature.

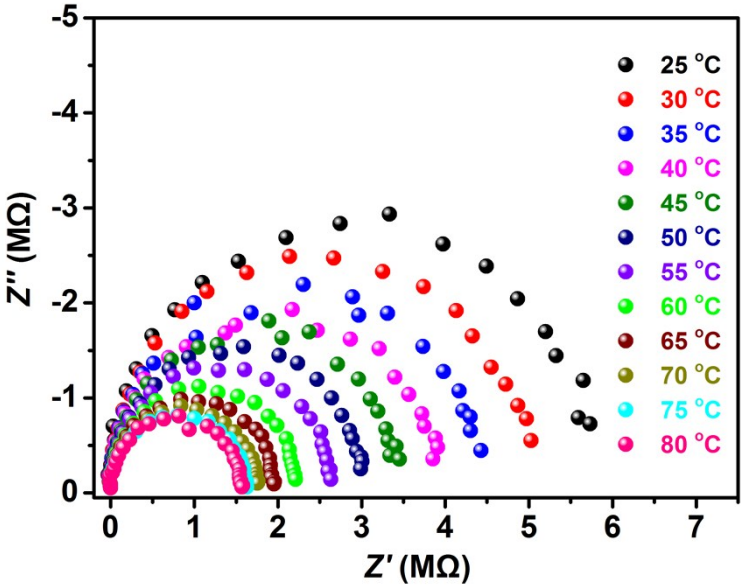

Figure S12 | Proton conductivity of **FJU-31@Bu** in anhydrous conditions at different temperature.

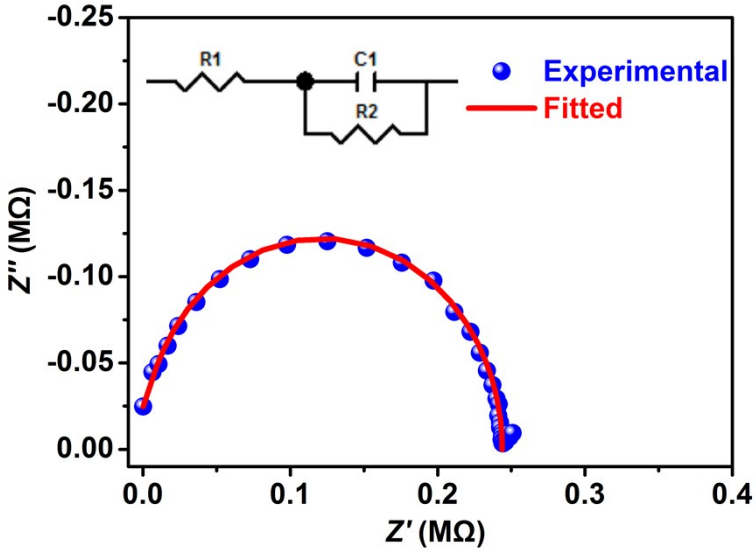

Figure S13 | Fitting for the Nyquist plot at 30°C in anhydrous conditions of **FJU-31@Hq**, with circuit model used for the data fitting shown as an inset.

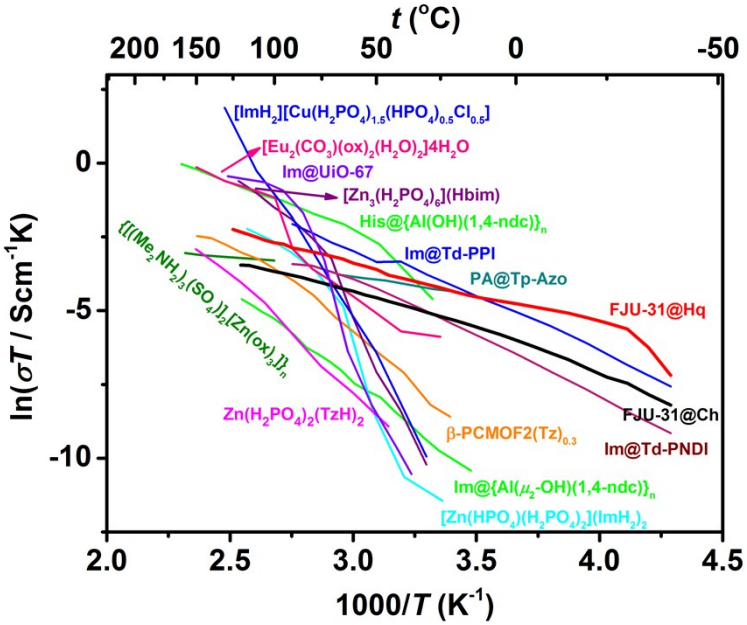

Figure S14 | Arrhenius plot for **FJU-31@Hq** and **FJU-31@Ch** in comparison with other representative crystalline porous proton-conducting materials under anhydrous conditions.

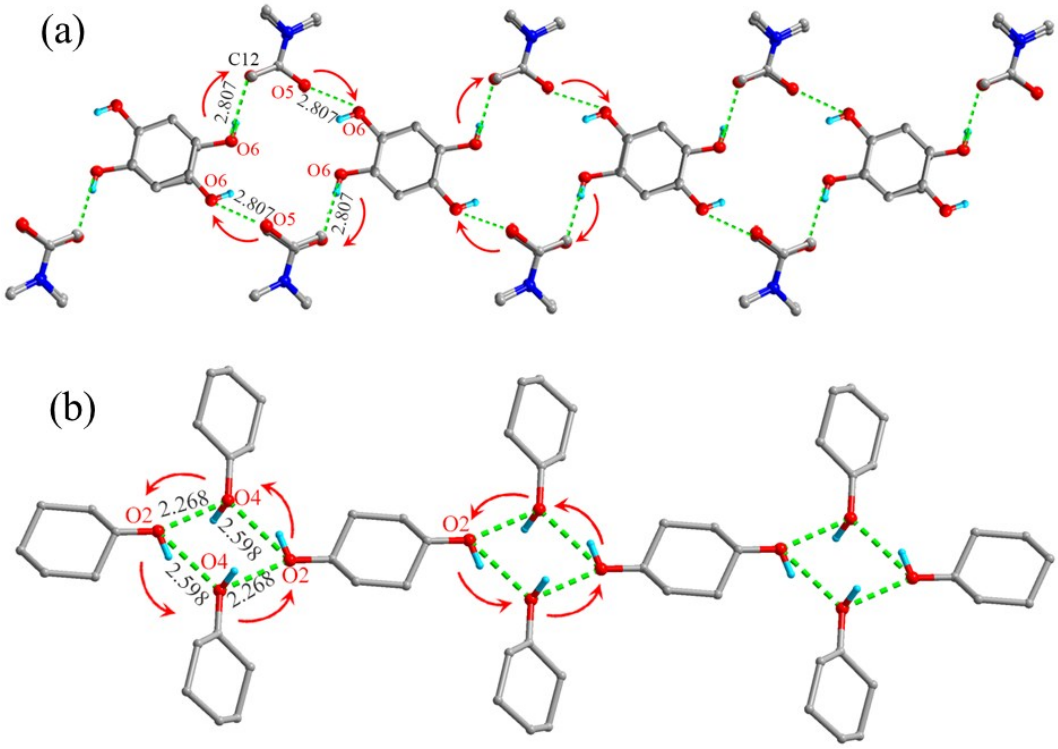

Figure S15 | Speculative proton pathway conduction for **FJU-31@Hq** (a) and **FJU-31@Ch** (b) based on single crystal X-ray data showing the actual positions of hydroquinone and DMAc or two types of cyclohexanol within the structure. The green dashed lines represent the hydrogen-bonding interactions between the hydroquinone and DMAc, or two types of cyclohexanol.

For **FJU-31@Hq** (**Figure S15a**), there is a large residual Q peak (1.58) located in the ortho-position of the hydroxyl group on hydroquinone, indicating the hydroxyl groups may be splitting. Meanwhile, the atoms of C12 and O5 show similar diffracted intensity and could not be completely distinguished by SCXRD, therefore they may substitute each other at the given site. According to the above analysis, the hydroquinone and DMAc molecules located in the channel could swing and roll over, and then to generate an orbicular intermolecular hydrogen-bonding interaction. Moreover, the proton H^+ ion from hydroquinone could pass from one end to the other end, so that the two kinds of guest molecules could made a complete proton conducting pathway in the channel for **FJU-31@Hq**. For **FJU-31@Ch** (**Figure S15b**), there are two types of cyclohexanol molecules. The hydroxyl group from one cyclohexanol molecule splits into two parts because the center of this cyclohexanol locates at the inversion center with the Wyckoff position 1*d*. The two types of cyclohexanol molecules could generate an intermolecular hydrogen-bonding interaction and then made a complete proton conducting pathway in the one-dimensional rhombic channel for **FJU-31@Ch**.

Supplementary References

1 H.-L. Zhou, R.-B. Lin, C.-T. He, Y.-B. Zhang, N. Feng, Q. Wang, F. Deng, J.-P. Zhang and X.-M. Chen. *Nat. Commun.*, 2013, **4**, 2534-2541.

2 C. D. Wu and W. B. Lin, *Angew. Chem., Int. Ed.*, 2005, **44**, 1958-1961; *Angew. Chem.,* 2005, **117**, 1994-1997.

3 G. Mehlana, G. Ramon and S. A Bourne, *CrystEngComm.*, 2014, **16**, 8160-8168.

4 S. Henke, A. Schneemann, A. Wuetscher and R. A. Fischer, *J. Am. Chem. Soc.*, 2012, **134**, 9464-9474.

5 A. Demessence and J. R. Long, *Chem. -Eur. J.*, 2010, **16**, 5902-5908.

6 C. Serre, F. Millange, C. Thouvenot, M. Nogues, G. Marsolier, D. Loueer and G. Ferey, *J. Am. Chem. Soc.*, 2002, **124,** 13519-13526.

7 Y.-Y. Liu, S. Couck, M. Vandichel, M. Grzywa, K. Leus, S. Biswas, D. Volkmer, J. Gascon, F. Kapteijn, J. F. M. Denayer, M. Waroquier, V. Van Speybroeck and P. Van Der Voort, *Inorg. Chem.*, 2013, **52**, 113-120.

8 Y.-S. Wei, K.-J. Chen, P.-Q. Liao, B.-Y. Zhu, R.-B. Lin, H.-L. Zhou, B.-Y. Wang, W. Xue, J.-P. Zhang and X.-M. Chen, *Chem. Sci.*, 2013, **4**, 1539-1546.

9 F. Salles, G. Maurin, C. Serre, P. L. Llewellyn, C. Knofel, H. J. Choi, Y. Filinchuk, L. Oliviero, A. Vimont, J. R. Long and G. Ferey, *J. Am. Chem. Soc.*, 2010, **132**, 13782-13788.

10 C. Mellot-Draznieks, C. Serre, S. Surble, N. Audebrand and G. Ferey, *J. Am. Chem. Soc.*, 2005, **127**, 16273-16278.

11 P. Horcajada, F. Salles, S. Wuttke, T. Devic, D. Heurtaux, G. Maurin, A. Vimont, M. Daturi, O. David, E. Magnier, N. Stock, Y. Filinchuk, D. Popov, C. Riekel, G. Ferey and C. Serre, *J. Am. Chem. Soc.,* 2011*,* **133***,* 17839-17847.

12 C. Serre, C. Mellot-Draznieks, S. Surblé, N. Audebrand, Y. Filinchuk and G. Ferey, *Science*, 2007, **315**, 1828-1831.

13 C. Serre, S. Surblé, C. Mellot-Draznieks, Y. Filinchuk and G. Ferey, *Dalton Trans.*, 2008, 5462-5464.

14 S. S. Nagarkar, S. M. Unni, A. Sharma, S. Kurungot and S. K. Ghosh, *Angew. Chem., Int. Ed.*, 2014, **53**, 2638-2642; *Angew. Chem.*, 2014, **126**, 2676-2680.

15 D. Umeyama, S. Horike, M. Inukai, Y. Hijikata and S. Kitagawa, *Angew. Chem., Int. Ed.*, 2011, **50**, 11706-11709; *Angew. Chem.*, 2011, **123**, 11910-11913.

16 Q. Tang, Y. Liu, S. Liu, D. He, J. Miao, X. Wang, G. Yang, Z. Shi and Z. Zheng, *J. Am. Chem.*

Soc., 2014, **136**, 12444-124449.

17 Y. Ye, L. Zhang, Q. Peng, G. Wang, Y. Shen, Z. Li, L. Wang, X. Ma, Q. H. Chen, Z. Zhang and S. Xiang, *J. Am. Chem. Soc.*, 2015, **137**, 913-918.

18. S. C. Liu, Z. F. Yue and Y. Liu, *Dalton Trans.*, 2015, **44**, 12976-12980.

19 D. Umeyama, S. Horike, M. Inukai and S. Kitagawa, *J. Am. Chem. Soc.*, 2013, **135**, 11345-11350.

20 S. Horike, D. Umeyama, M. Inukai, T. Itakura and S. Kitagawa, *J. Am. Chem. Soc*., 2012, **134**, 7612-7615.

21 T. Panda, T. Kundu and R. Banerjee, *Chem. Commun.*, 2013, **49**, 6197-6199.

22 W.-X. Chen, H.-R. Zhuang, G.-L. Xu, L.-S. Long, R.-B. Huang and L.-S. Zheng, *Chem.Commun.*, 2011, **47**, 11933-11935.

23 J. A. Hurd, R. Vaidhyanathan, V. Thangadurai, C. I. Ratcliffe, I. L. Moudrakovski and G. K. H. Shimizu, *Nat. Chem.*, 2009, **1**, 705-710.

24 D. Umeyama, S. Horike, M. Inukai, T. Itakura and S. Kitagawa, *J. Am. Chem. Soc.*, 2012, **134**, 12780-12785.

25 S. Bureekaew, S. Horike, M. Higuchi, M. Mizuno, T. Kawamura, D. Tanaka, N. Yanai and S. Kitagawa, *Nat. Mater.*, 2009, **8**, 831-836.

26 M. Inukai, S. Horike, W. Chen, D. Umeyama, T. Itakura and S. Kitagawa, *J. Mater. Chem. A.*, 2014, **2**, 10404-10409.

27 S. Horike, W. Chen, T. Itakura, M. Inukai, D. Umeyama, H. Asakura and S. Kitagawa, *Chem. Commun.*, 2014, **50**, 10241-10243.

28 S. Chandra, T. Kundu, S. Kandambeth, R. BabaRao, Y. Marathe, S. M. Kunjir and R. Banerjee, *J. Am. Chem. Soc.*, 2014, **136**, 6570-6573.

29 M. Inukai, S. Horike, D. Umeyama, Y. Hijikata and S. Kitagawa, *Dalton Trans.*, 2012, **41**, 13261-13263.

30 J. M. Taylor, K. W. Dawson and G. K. H. Shimizu, *J. Am. Chem. Soc.*, 2013, **135**, 1193-1196.

31 A. Shigematsu, T. Yamada and H. Kitagawa, *J. Am. Chem. Soc.*, 2011, **133**, 2034-2036.

32 (a) R. C. T. Slade, A. Hardwick and P. G. Dickens, *Solid State Ionics*, 1983, **9***,* 1093-1098; (b) G. Alberti and M. Casciola, *Solid State Ionics*, 2001, **145**, 3-16.

33 E. Pardo, C. Train, G. Gontard, K. Boubekeur, O. Fabelo, H. Liu, B. Dkhil, F. Lloret, K. Nakagawa, H. Tokoro, S. Ohkoshi and M. Verdaguer, *J. Am. Chem. Soc.*, 2011*,* **133***,* 15328-15331.

34 V. G. Ponomareva, K. A. Kovalenko, A. P. Chupakhin, D. N. Dybtsev, E. S. Shutova and V. P.

Fedin, *J. Am. Chem. Soc.*, 2012, **134**, 15640-15643.

35 W. J. Phang, H. Jo, W. R. Lee, J. H. Song, K. Yoo, B. S. Kim and C. S. Hong, *Angew. Chem., Int. Ed.*, 2015, **54**, 5142-5146; *Angew. Chem.*, 2015, **127**, 5231-5235.

36 S. C. Sahoo, T. Kundu and R. Banerjee, *J. Am. Chem. Soc.*, 2011, **133**, 17950-17958.

37 T. Yamada, M. Sadakiyo and H. Kitagawa, *J. Am. Chem.Soc.*, 2009, **131**, 3144-3145.

38 M. Yoon, K. Suh, H. Kim, Y. Kim, N. Selvapalam and K. Kim, *Angew. Chem., Int. Ed*., 2011, **50**, 7870-7873; *Angew. Chem.*, 2011, **123**, 8016-8019.

39 M. Sadakiyo, T. Yamada and H. Kitagawa, *J. Am. Chem. Soc.*, 2009, **131**, 9906-9907.

40 (a) J. Seo, C. Bonneau, R. Matsuda, M. Takata and S. Kitagawa, *J. Am. Chem. Soc.*, 2011, **133**, 9005-9013; (b) J. P. Zhang, S. K. Ghosh, J. B. Lin, and S. Kitagawa, *Inorg. Chem.*, 2009, **48**, 7970-7976.

41 Z. Q. Jiang, G. Y. Jiang, F. Wang, Z. Zhao and J. Zhang, *Chem.-Eur. J.*, 2012, **18**, 10525-10529.